Logjams and channel morphology influence sediment storage, transformation of organic matter, and carbon storage within mountain stream corridors

Nicholas A. Sutfin[1,2*], Ellen Wohl[1], Timothy Fegel[3], Natalie Day[4], Laurel Lynch[5]

[1]*Department of Geosciences, Colorado State University, Fort Collins, CO 80523-1482*
[2]*Integrated Water, Atmosphere, and Ecosystem Education and Research Program, Colorado State University*
[3]*Rocky Mountain Research Station, United States Forest Service, Fort Collins, CO 80526*
[4]*United States Geological Survey, Colorado Water Science Center, Lakewood, CO*
[5]*Department of Soil and Water Systems, University of Idaho, Moscow, ID 83844*
[*]Corresponding author current affiliation: Department *of Earth, Planetary, and Environmental Sciences, Case Western Reserve University, Cleveland, OH 44106*

Key Points

- Less confined valleys store relatively more carbon in floodplain fine sediment and large wood than more confined valley segments
- Channels with single thread planforms store more carbon than more complex systems with multiple channels of flow in wide valley bottoms
- Logjam abundance is linked to shallower fine sediment depth and microbial transformation of organic matter in complex multithread reaches

Abstract

The flow of organic matter (OM) along rivers, and retention within floodplains, contribute significantly to terrestrial carbon storage and ecosystem function. Carbon storage and ecosystem processing of OM largely depend upon hydrogeomorphic characteristics of streams and valleys, including channel geometry and the connectivity of water across and within the floodplain. To examine the role of river morphology on carbon dynamics in mountain streams, we (1) quantify organic carbon (OC) storage in fine sediment, litter, and wood along 24 forested gravel-bed stream reaches in the Rocky Mountains of CO, U.S.A., (2) examine morphological factors that regulate sediment and OC storage (e.g., width, slope, logjams), and (3) utilize fluorescence spectroscopy to examine how the composition of OM in surface water and floodplain fine sediment is influenced by channel morphology. Multivariate regression of the study reaches, which have varying degrees of confinement, slope, and elevation, indicates that

OC storage per area is higher in less confined, in lower-gradient stream reaches, and at higher elevations. We find that limited storage of fine sediment and microbial OC transformation within multithread channels decrease storage per area (252±39 Mg C ha^{-1}) relative to single-thread channel reaches (346±177 Mg C ha^{-1}) in relatively unconfined valleys. We posit that positive feedbacks between channel morphology and persistent channel-spanning logjams that divert flow into multiple channels limit the aggradation of floodplain fine sediment. Because multithread stream reaches are hotspots for the transformation of OM they are less effective OC reservoirs, but they are important sources for food webs in aquatic ecosystems.

Plain Language Summary

The organic byproducts of living material including plants, insects, and microbes (organic matter) are important components of healthy ecosystems in mountain streams and provide carbon storage, which prevents CO_2 from entering the atmosphere. Carbon storage and the breakdown of organic matter by ecosystems in rivers is influenced by the shapes of river channels and valleys. To examine how the storage of organic matter are influenced by valley and channel geometry, we (1) survey 24 streams in the Colorado Rocky Mountains and collect soil samples to estimate carbon storage, (2) examine differences in carbon storage associated with the shapes of stream channels and valleys, and (3) examine the differences in the molecular structure of organic matter associated with differences in valley and channel shape. We find that storage per area is higher in wider valleys, lower gradient streams, and higher elevations. Streams with numerous channels of flow across wide valley bottoms store shallower fine sediment and less carbon compared with streams in wide valleys. These complex multithread streams facilitate the

57 breakdown of carbon by microbes making them less efficient reservoirs for organic carbon
58 storage but serving important functions for healthy ecosystems.
59
60
61
62 **1 Background**
63 Rivers play a significant role in terrestrial carbon budgets through release of OC to the
64 atmosphere, delivery to oceans (Aufdenkampe et al., 2011; Galy et al., 2015), and storage in
65 downed, dead wood and floodplain soil (N. A. Sutfin et al., 2016). Combined OC storage in the
66 atmosphere and biosphere is less than storage in soils (Falkowski et al., 2000), which have the
67 potential to retain OC at depth along river corridors (Ricker & Lockaby, 2015; D'Elia et al.,
68 2017; Omengo et al., 2018). Because the highest uncertainty in annual exchanges of carbon
69 between the atmosphere, surface ocean, and land surface occurs within terrestrial reservoirs
70 (Gregory et al., 2009; Ballantyne et al., 2012), OC dynamics and storage along river floodplains
71 could represent a substantial component of global carbon budgets.
72 Although large, lowland rivers have extensive floodplains that can store OC, smaller
73 streams constitute ~95% of global river length and therefore make important contributions to
74 carbon dynamics (Downing et al., 2012). Allochthonous (terrestrially-derived) organic matter
75 (OM) inputs in headwater streams are the foundation of food webs and are crucial for fisheries
76 and autochthonous (in-stream) primary production in larger rivers (Vannote et al., 1980; Chapin
77 et al., 2011) (we use OC when discussing storage reservoirs of organic carbon (Mg C ha^{-1}) and
78 OM when discussing specific sources of OC and the decomposition or transformation of those
79 sources by microbial communities and aquatic invertebrates). Floodplains along 1^{st}, 2^{nd}, & 3^{rd}

order mountainous headwater streams have been shown to contain higher soil OC content than adjacent uplands (Wohl et al., 2012; Sutfin & Wohl, 2017) and can store more OC per area than higher-order lowland rivers (N. A. Sutfin et al., 2016). We focus on these smaller streams to examine controls on OC dynamics within river corridors.

Determining whether OC retention within floodplains constitutes long-term C storage requires considering (1) the duration of floodplain fine sediment storage prior to downstream transportation, and (2) the potential for OM decomposition and mineralization to the atmosphere. Geomorphic response to floods regulates the duration of sediment storage (Sutfin & Wohl, 2019) and hydrologic connectivity regulates decomposition of OM (Raymond et al., 2016; Wollheim et al., 2018). Thus, the potential for OC storage along river corridors is highly sensitive to hydrological condition and valley and channel geometry.

Biophysical factors that influence channel geometry and hydrologic connectivity include in-stream wood, logjams, beaver ecosystem engineering, vegetation, valley width and confinement, and hydrologic flow and sediment regimes, which together create and maintain channel complexity (Polvi and Wohl, 2013; Livers & Wohl, 2016). Here, channel complexity captures the presence and variability of diverse channel geometry, including planform and bedforms; greater channel complexity equates to increased spatial variability in channel geometry (Livers & Wohl, 2016). Increased channel complexity is more common along headwater streams as a result of limited human impact and prevalent biotic drivers of channel morphology (i.e., logjams, beavers) (Polvi & Wohl, 2013; Beckman & Wohl, 2014). While complex headwater streams may have a higher capacity to store OC (Wohl et al., 2012; Sutfin et al., 2016), they may also act as hotspots of OM decomposition, where longer water residence times (Gooseff et al., 2007) provide greater opportunities for microbial metabolism (Battin et al.,

2008). Recent work shows that the composition of OM flowing through complex channel segments is more molecularly diverse than that of single-thread channels; these differences become increasingly pronounced as seasonal declines in flow reduce hydrologic connectivity across the floodplain (Lynch, et al., 2019). The degree to which higher channel complexity corresponds to enhanced OC storage versus decomposition and mineralization remains poorly constrained.

Here, we (1) quantify differences in OC storage per area along valley segments with varying channel and valley geometry, (2) identify potential hydrogeomorphic mechanisms underlying differences in OC storage, and (3) examine longitudinal trends in the composition of OM as it cycles through surface waters and adjacent floodplains. To *quantify OC storage*, we surveyed and sampled *24 relatively undisturbed study reaches* with similar geology (Braddock & Cole, 1990) and climate (Birkeland et al., 2003) spanning an ecotone and vegetation shift (Veblen & Donnegan, 2005; Polvi et al., 2011) along the tributaries and main stem of four headwater streams of the South Platte River basin in northern Colorado. Six years of *logjam presence surveys at nine of the 24 study reaches* complement morphology surveys to examine the role of logjams on sediment and OC storage. Two of the 24 study reaches were extended in length, creating *intensive study sites* that we used to investigate the role of channel geometry and logjams on OM transformation in surface waters and floodplain fine sediment.

2 Study Area

Located within and around Rocky Mountain National Park and the Arapaho and Roosevelt National Forests, we surveyed 24 study reaches located in the Subalpine and Montane zones of nested tributaries within North Saint Vrain Creek (NSV), Glacier Creek (GCK), South

Fork of the Poudre River (SFP), and the Big Thompson River (BTR) watersheds (Figure 1). Smaller tributaries include Ouzel, Cony, Hunters, and Mills Creeks.

2.1 Geological setting

The geology and glacial history of the study area within the Colorado Front Range (CFR) of the Rocky Mountains regulates valley morphology, but does not directly influence OC inputs to the study reaches. The underlying lithologic core of the Colorado Front Range (CFR) is composed of Precambrian gneiss, schist, granite, and other igneous rocks primarily of intrusive origin (Braddock & Cole, 1990). Irregular bedrock jointing facilitates longitudinal variability in the relative confinement of stream valleys, such that broader valleys commonly coexist with more closely spaced bedrock joints and strath terraces along otherwise confined, narrower valleys (Wohl, 2008). Pleistocene alpine terminal moraines extend eastward down-valley to elevations of approximately 2,300 to 2,500 m and play a significant role in shaping the relative confinement of valleys among study reaches. On the eastern side of the CFR, knickpoints at approximately 2,000 m in elevation mark the transition from broader glaciated valleys to narrow incised valleys in sedimentary rocks at the eastern margin of the Precambrian core (Anderson et al., 2006). Broader valleys typically have pool-riffle or plane bed channel morphology (Montgomery & Buffington, 1997; Livers & Wohl, 2015), whereas more confined valleys are more likely to have cascade or step-pool morphology, including both boulder and logjam-forced steps.

2.2 Climate and vegetation

Distinct vegetation zones reflect differences in precipitation patterns and fire regimes (Veblen & Donnegan, 2005) that influence hydrologic flow paths and OM inputs to streams and

floodplains. Vegetation in the study area reflect changes across the ecotone from montane to subalpine forests in the CFR. At 1,830 m elevation, grassland steppe vegetation transitions into montane forest, which is dominated by ponderosa pine (*Pinus ponderosa var. scopulorum*) and Douglas-fir (*Pseudotsuga menziesii*) extending to ~2,750 m. The Montane zone receives ~75 cm of annual average precipitation in the eastern CFR between (record spanning 1981 to 2010; PRISM Climate Group, 2012) and experiences relatively frequent and low severity ground fires approximately every 30-100 years (Veblen & Donnegan, 2005). Forests in the Subalpine zone, extending from ~2,750 to 3,400 m, are dominated by subalpine fir (*Abies lasiocarpa*), lodgepole pine (*Pinus contorta*), limber pine (*Pinus flexilis*), Engelmann spruce (*Picea englemannii*), and aspen (*Populus tremuloides*) (Veblen & Donnegan, 2005). Large stand-replacing fires occur on average every 500 years in the Subalpine zone, where annual average precipitation is ~85 cm (Barry, 1973; Birkeland et al., 2003; PRISM Climate Group, 2012). Vegetation within the riparian zone typically corresponds to that of respective upland vegetation with additions of blue spruce (*Picea pungens*); in the Subalpine zone Douglas fir, Engelmann spruce, and aspen are abundant. Willow (*Salix* spp.), sedges (*Carex* spp.), and river birch (*Betula fontinalis*) are present at sites with relict beaver activity (Veblen & Donnegan, 2005; Polvi et al., 2011).

2.3 Hydrological condition

The rivers and streams of the CFR are snowmelt dominated and typically have a single annual hydrograph peak during June, and sometimes the last week of May. Paleoflood indicators and estimates of flood magnitudes in the CFR (McCain & Shroba, 1979; Jarrett, 1990) suggest the high intensity storms (typically from July to September) at elevations below 2,300 m disproportionately influence stream discharge at lower elevations within and below the Montane

zone. Hydrologic response to these storms sometimes results in secondary peak flows that exceed the snowmelt-dominated peak (Jarrett, 1990). One such event occurred during the period in which this study was taking place.

On September 11th to September 13th, 2013, a prolonged extreme precipitation event broke several rainfall records in the state of Colorado (Gochis et al., 2014) and resulting floods restructured floodplains in much of the CFR (Yochum & Collins, 2015; Yochum et al., 2017; Sholtes et al., 2018). Estimated recurrence intervals of peak discharge in rivers and streams in the CFR during the event ranged from 5-year to >100-year flow events (Yochum & Collins, 2015). Most of our study reaches were located outside the center of the highest rainfall accumulations, and received somewhere between ~100-250 mm of rain equating to 10-year to 500-year precipitation events (Gochis et al., 2014). However, the lower portion of North Saint Vrain Creek was located in the center of the storm, which received ~380-520 mm of rainfall, and four study sites were heavily impacted.

Estimates of peak discharge in streams and rivers of the CFR during the 2013 storm do not include values for North Saint Vrain Creek at Allenspark, but estimates of sediment residence time provide context for the recurrence interval of the flood. The USGS stream gauge on North St. Vrain Creek near Allenspark, CO (gauge # 6721500) – downstream of 11 and upstream of 4 of our study reaches – was no longer active in the 2013 flood, but discontinuous records of flow (1926 to 1930 and 1987 to 1997) indicate a daily mean annual discharge of 1.56 $m^3 s^{-1}$ and a maximum annual peak discharge of 13.30 $m^3 s^{-1}$. Yochum and Collins (2015) estimate that flow at the N. St. Vrain Creek, Allenspark gauge was greater than a 2-year flood. However, floodplain fine sediment samples collected at two sites below the USGS Allenspark gauge before the flood estimated a floodplain sediment residence time of >600 y BP (Sutfin and

195 Wohl, 2019). Evacuated of floodplain fine sediment at these two study reaches during the 2013
196 flood suggests a recurrence interval >500 years. Pre-and post-flood lidar differences and
197 sediment coring of the Ralph Price Reservoir downstream quantified ~100 years of erosion along
198 the lower North Saint Vrain Creek corridor and a substantial loss of OC storage during the event
199 (Rathburn et al., 2017).

200 Stream gauges in the study area lack continuous discharge data of sufficient length to
201 estimate recurrence intervals with meaningful certainty, but can provide context for annual
202 trends, seasonal patterns in discharge, and the magnitude of the 2013 event. The USGS gauge
203 (#402114105350101) on the Big Thompson River at Moraine Park located downstream of 8 of
204 our study reaches and upstream of Estes Park provides 17 discontinuous years of streamflow
205 between 1996 and 2020. This gauge recorded an annual mean of 1.6 $m^3 s^{-1}$ and a mean annual
206 maximum of 17 $m^3 s^{-1}$ for the period of record. Annual peak flows within this period of record
207 occurred in June or the last week of May, with two exceptions. An annual peak discharge of 28.9
208 $m^3 s^{-1}$ occurred on 9 July, 2011, and an annual peak discharge of 32 $m^3 s^{-1}$ occurred on 12
209 September, 2013, during the 2013 extreme precipitation event.

210

211 *2.4. Channel morphology and OC retention in the CFR*

212 Past work suggests that valley geometry largely controls sediment storage in floodplain
213 sediments within the study area. The geomorphic impact of the 2013 floods in the CFR
214 suggested that valley confinement and overbank stream power, which were significantly lower in
215 glaciated valleys, were among the strongest predictors for floodplain sediment residence times
216 (Sutfin & Wohl, 2019). Unconfined glaciated valleys attenuate flood waves by allowing flows to
217 spread across the floodplain, which dissipates energy, decreases flow velocity, and decreases

sediment transport capacity. Sediment residence times were also significantly shorter in the Montane zone than in the Subalpine zone (Sutfin & Wohl, 2019), both of which are characterized by distinctly different forest types and fire regimes (see section 2.2).

Channel morphology and OC retention in the CFR are also influenced by large wood (>10 cm in diameter and >1 m in length) and logjams. Streams in the CFR are dominated by cobble to boulder substrate, but transitional morphological states in channel form occur in response to altered wood regimes and reduced logjam occurrence (Livers et al., 2018). Instream wood loads and spacing of channel spanning logjams are regulated by variability in forest age and valley geometry (Wohl and Cadol, 2011). While large wood is a substantial component of OC storage in fluvial corridors of the CFR, logjams also facilitate OM retention (Beckman & Wohl, 2014). Prior work also suggested that logjam-forced multithread channels increased OC storage per area in the CFR (Wohl et al., 2012), but that prior study was based on a limited number of study sites. In quantifying OC storage in floodplains of the CFR and identifying potential drivers of differences among channel and valley types, we examine if and why logjam-induced multithread channels store more OC per area than other channel types.

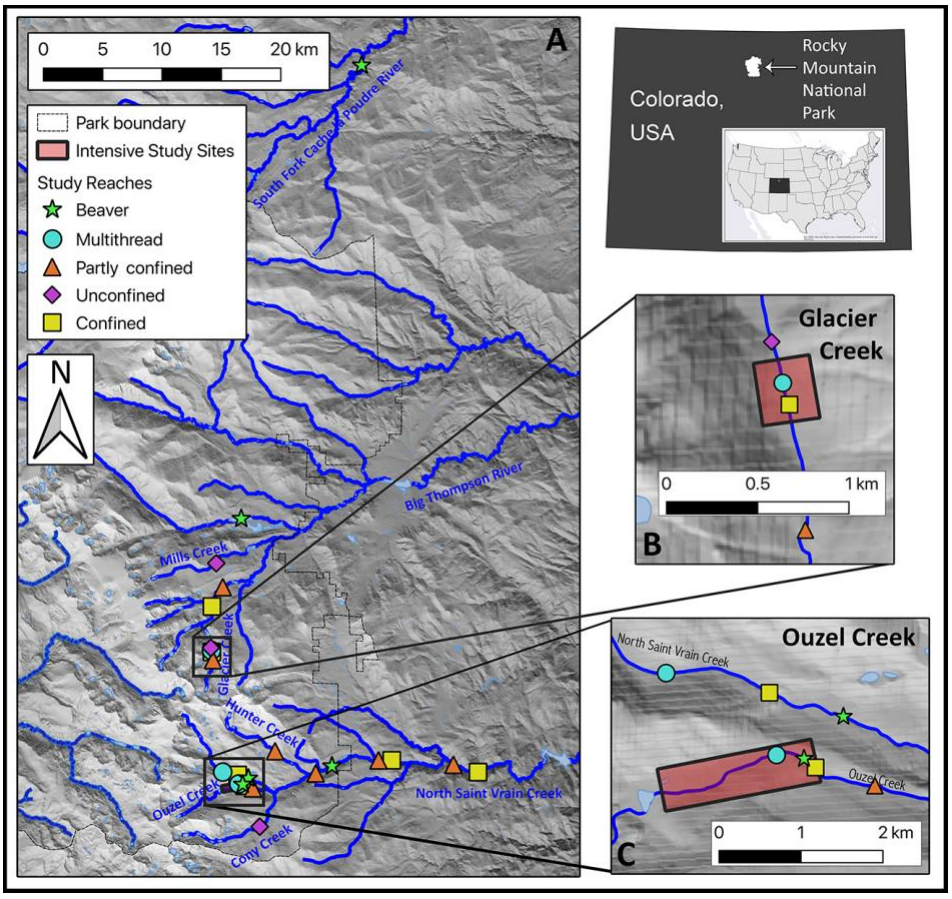

Figure 1. Map of the study area along the Colorado Front Range of the Rocky Mountains, U.S. Twenty-four study reaches representing five different channel types (A) are indicated in the legend. Large rectangles with bold outlines identify intensive study sites that capture transitions in channel complexity (single-multiple-single thread reaches) on Glacier Creek (B) and Ouzel Creek (C). At these intensive study sites, organic matter composition was examined along transitions in valley confinement using fluorescence spectroscopy. Logjam surveys were conducted in the N. Saint Vrain Creek Basin upstream of the Rocky Mountain National Park boundary.

3. Methods

In the following subsections, we describe several data sets and analyses including field observations, sample collection and analysis, GIS analysis, and statistical modeling to ask, "How does valley and channel morphology influence floodplain OC storage in the Colorado Front Range?". To *quantify differences in OC storage per area* we describe below *24 study reaches* and methods for evaluating valley and channel morphology, surveying floodplain topography

and sediment depth, calculating sediment volume (GIS), collecting litter and soil samples, surveying large wood on the floodplain, analyzing OC content, and quantifying OC storage along diverse channel types (sections 3.1 to 3.5). To identify potential hydrogeomorphic mechanisms for differences in OC storage along valley segments with varying channel and valley geometry we also present *six years of logjam absence/presence surveys* within a watershed encompassing nine of the 24 study reaches (section 3.6). Two of the 24 study reaches were selected as intensive study sites and extended in length to include additional upstream and downstream reaches. Floodplain sediment and surface water samples were collected for *detailed analysis of OM composition at the two intensive study sites* to examine the role of channel morphology on OC molecular diversity and fate (section 3.7). A salt tracer application was conducted to calculate discharge within each study reach of the two intensive study sites during the time of sample collection (section 3.8).

3.1 Study reach selection

We characterize study reaches by relative channel complexity and degree of valley confinement. We classify study reaches as abandoned or active beaver meadows based on field evidence of exposed or buried beaver dams and ponds, beaver-dug canals, beaver lodges, beaver mounds and slides, and beaver chewed trees (Ives, 1942; Polvi & Wohl, 2012, 2013). Within the CFR, old-growth forests (> 200 years old) include trees that are large enough to create persistent channel-spanning logjams. Where logjams persist for a year or more, diversion of flows can form secondary channels and sometimes multiple channels of flow across relatively unconfined valley bottoms. We refer to these complex channel segments, where evidence of beavers is not present, as *multithread channels*.

Stream reaches that are not multithread and lack evidence of beaver activity are classified using a valley confinement ratio (C_r), calculated as the stream channel width divided by the valley width. Stream reaches bounded entirely by bedrock and with the absence of a floodplain were considered extremely confined and were not included in the study. Reaches with $C_r > 0.5$ are classified as *confined* because a valley less than two times the width of the channel does not have space to accommodate channel avulsions or side channel development. Those with a ratio between 0.5 and 0.24 are defined as *partly confined* because overbank channels can be observed in these valleys, but multithread channels do not occur. Valleys with $C_r < 0.24$ are defined as *unconfined* valleys because these valleys accommodate the development of side channels, channel avulsions, and multithread channel systems.

This classification result in five valley reach types including three classes in relatively *unconfined valleys* (beaver meadows, multithread channels, and unconfined reaches) and two classes in relatively *narrow valleys* (partly confined and confined reaches) (Table 1).

Table 1
Physical attributes of the 24 study reaches.

Stream	Valley type	Mean valley width (m)	Mean channel width (m)	Mean valley confinement (m/m)	Mean gravimetric soil moisture content (%)	Stream Gradient (%)	Elevation (m)	Drainage Area (km2)
NSV	Confined	18	13.0	0.73	16	0.032	2385	97.7
Ouzel	Confined	9	5.3	0.55	35	0.095	2971	10.7
GCK	Confined	12	8.5	0.32	34	0.13	2845	21.0
NSV	Confined	11	6.2	0.58	38	0.085	2951	17.9
NSV	Confined	19	14.1	0.74	20	0.026	2162	205.1
GCK	Confined	10	5.6	0.50	42	0.09	3071	9.7
NSV	Partly confined	33	17.1	0.45	21	0.037	2420	96.4
Ouzel	Partly confined	14	5.1	0.34	38	0.063	2927	11.1
GCK	Partly confined	33	8.5	0.26	25	0.027	2701	33.2
Hunters	Partly confined	15	3.7	0.24	30	0.069	3013	10.1
NSV	Partly confined	27	12.7	0.45	23	0.023	2226	200.5
GCK	Partly confined	14	4.2	0.28	34	0.02	3118	7.1

NSV	Partly confined	43	14.5	0.31	48	0.016	2573	77.4
Cony	Unconfined	26	5.6	0.21	58	0.028	3054	12.7
GCK	Unconfined	32	5.1	0.15	54	0.013	3053	10.3
Mills	Unconfined	47	7.8	0.10	41	0.01	2797	3.0
NSV	Beaver	67	6.8	0.10	55	0.037	2901	19.1
Ouzel	Beaver	43	7.0	0.13	65	0.04	2978	10.6
NSV	Beaver	247	14.1	0.05	40	0.012	2547	82.2
BTR	Beaver	180	17.3	0.09	29	0.006	2462	93.7
SFP	Beaver	77	10.6	0.13	25	0.011	2410	180.6
NSV	Multithread	61	6.5	0.10	44	0.063	3035	14.8
GCK	Multithread	34	6.7	0.18	39	0.03	3068	9.8
Ouzel	Multithread	53	5.2	0.10	53	0.033	2990	10.5

Note: Reach abbreviations include BTR = Big Thompson River, GCK = Glacier Creek, NSV = North Saint. Vrain Creek, SFP = South Fork Cache La Poudre River

287

288 *3.2 Field surveys and soil sampling for OC storage*

289 Field surveys were conducted and the depth of floodplain fine sediment was measured
290 (summer 2012, 2013, 2014) along each of the 24 study reaches. Study reaches were defined by
291 11 surveyed transects spaced approximately one bankfull width apart and oriented orthogonally
292 to the down-valley direction. A stadia rod and a laser rangefinder with 10-cm accuracy (Laser
293 Technologies®, TruPulse 360B) were used to survey topography along each transect at breaks in
294 slope and other points of interest (e.g., changes in grain size, transitions in vegetation type) with
295 a maximum spacing of 11 m between survey points. The depth of the underlying floodplain fine
296 sediment (< 2 mm) was measured at each survey point when a 1-cm diameter soil probe was
297 inserted into the floodplain surface. The probe was pounded into the surface using a 1.4 kg
298 sledgehammer until refusal at bedrock or coarser pebble and cobble material. Dominant
299 vegetation (e.g., grasses, willows, tree cover) and primary tree types (e.g., blue spruce, aspen,
300 subalpine fir) were noted at survey points along each transect to verify typical vegetation type
301 but were not used in statistical models. Approximate bankfull channel width was determined
302 between points along each transect using the height of depositional features that included point

bars and changes in vegetation as primary bankfull indicators. The stream gradient was measured using a survey of the estimated bankfull stage on the banks along the length of each study reach. Contributing drainage area for each study reach was calculated using 10 m resolution USGS digital elevation models (DEMs) in ESRI ArcMap. The elevation of each reach was taken as the elevation from the DEMs at the downstream transect along each study reach. Stream gradient was calculated as the slope of the linear regression line fit to all surveyed stream gradient points described above.

Soil sample locations were selected by systematic random sampling along each transect (Figure S1). Bootstrap analysis indicated that the variance and bias of the estimated mean OC content (for the entire depth of the sediment sampled at 15-cm increments) declined rapidly with an incremental increase in sample size until it leveled off at 11 sampling locations (Sutfin & Wohl, 2017). Bias was not further reduced until >30 sampling locations were included. We used these findings as guidance, and randomly selected single sampling location along each of the eleven transect of all study reaches to examine variability in OC content. The distance of each transect across the valley bottom was measured and potential sample locations were represented by 1-m increments that spanned the distance along the transect. A random number generator was used to select a distance from the valley edge for each sample location. Locations falling within the active channel were shifted to the first meter on the left or right riverbank by random selection. Locations that fell on bedrock resulted in a new random selection without replacement. When only bedrock was present along cross sections, no sediment samples were collected, although litter and duff was collected if present.

Sediment and litter and duff were collected at each sampling location where present. A 7-cm diameter cylindrical sampling tube was used to collect volumetric samples of OM in the O-

horizon as a single sample at each sampling location. A 7-cm diameter stainless steel hand auger was used to sample fine sediment at increments of 15-cm depth until refusal at bedrock or material exceeded ~2 mm in diameter. Auger length prevented sample collection at depths greater than 180 cm, which occurred at three sampling locations (660 sediment samples were collected at 273 sampling locations in total).

Twenty-one volumetric soil samples were collected in small pits excavated along the floodplain to estimate bulk density. A 7-cm diameter soil sampling tube was inserted horizontally and centered at ~5, 15, and 45-cm depth where roots did not interrupt sampling (Supplemental Table S1).

3.3 Analysis of OC content

Mineral soil samples were collected from the 24 study reaches and frozen until analysis for OC content by the Colorado State University, Soil and Water Testing Laboratory. An aliquot of each sample was dried for 48 hours at 60ºC, then ground and analyzed for total C and N by dry combustion (LECO 1000 CHN analyzer, LECO Corporation, St. Joseph, MI, USA). Each sample was treated with 0.4 N HCl and the CO_2 loss was measured gravimetrically to determine inorganic carbon content (CO_3-C). Soil OC content was calculated as total carbon minus CO_3-C. The gravimetric soil moisture content was determined as the difference between the mass of field-moist soil before and after it was dried at 105°C for 24 hours.

A total of 281 O-horizon samples were processed for OC content. Recognizable plant material (< 6 mm diameter, including litter and needles) and duff (unrecognizable and fragmented material between the litter and mineral soil layers, FIA, 2019) were dried at 105°C

for 24 hours. OC content of the combined O-horizon (litter + duff, hereafter referred to as 'litter') was estimated as 50% of the mass lost through loss on ignition at 550°C after 24 hours.

3.4 Organic Carbon storage as floodplain large wood

Wood surveys were conducted across the entire floodplain surface of each of the 24 study reaches to estimate OC storage in large wood. The length and diameter of all floodplain wood (greater than 1 m in length and 10 cm in diameter) were measured and wood volumes were calculated as the volume of a cylinder using the average diameter of the two end measurements. The mass of C stored in each large wood piece was estimated using a calculated average density for species in the study area (Douglas fir, lodgepole pine, ponderosa pine, Engelmann spruce, and aspen) of 400 kg m^{-3} (Glass & Zelinka, 2004) and assuming 50% C by mass.

3.5 Organic Carbon storage in wood, litter, and sediment

Total OC storage was calculated in three compartments (i.e., sediment, wood, and litter) for each of the 24 study reaches and presented as the mass of OC per floodplain area.

The mass of OC stored in fine sediment at each study reach was estimated using soil samples, depth measurements, and GIS. The volume of floodplain fine sediment was calculated using measured depths of fine sediment and triangular irregular networks (TINs) in ESRI ArcMap. Sediment volumes were multiplied by the average bulk density across study reaches (ρ_b = 0.9 ± 0.24 g cm^{-3}, Supplemental Table S1), to estimate the mass of floodplain fine sediment along each study reach. Observed inconsistent changes in soil OC content with depth likely resulted from dynamic and spatially discontinuous erosion and sedimentation events across the floodplains. Heterogeneity of floodplain architecture results in poorly defined soil profiles and

371 buried lenses of organic-rich sediment present at some study reaches. Because these lenses were
372 small isolated features, interpolation across the floodplain would result in overestimates of OC
373 content. Instead, depth-averaged OC content of systematic randomly sampled sediment
374 (described in section 3.2) was used to calculate reach-average OC content. The total mass of fine
375 sediment along each study reach was multiplied by the mean gravimetric OC content along each
376 reach to calculate the total mass of OC storage in floodplain sediment.
377 The mass of OC storage as litter was estimated using an average litter depth, OC content,
378 and bulk density. The average depth of the litter layer was multiplied by the floodplain surface
379 area – generated from TINs as described above – to estimate O-horizon volumes in each reach.
380 Litter mass (calculated as the average bulk density multiplied by the volume of litter) was
381 multiplied by the average OC content to estimate the mass of OC storage in litter for each reach.
382 The total mass of OC in all floodplain reservoirs (i.e., wood, sediment, litter) was divided
383 by the surface area of each TIN to estimate total OC storage per area along each study reach.
384
385 *3.6 Instream logjam surveys and fine sediment depth*
386 We utilized an ongoing presence-absence survey of logjams in the North St. Vrain Creek
387 watershed to examine relationships between logjams and the depth of floodplain fine sediment at
388 nine of the 24 study reaches. The number of instream logjams was monitored and recorded
389 annually over a six-year period from 2010 to 2015 (Supplemental Table S2). Locations of
390 logjams upstream of the Pleistocene terminal moraine – located at approximately 2,500 m
391 elevation – were recorded using a handheld GPS unit. Logjams that fell within the ESRI ArcMap
392 shapefile extent of the surveyed study reach, plus one channel width up and down valley of each
393 study reach, were counted for each year. We estimated mean floodplain fine sediment depth by

394 dividing the floodplain sediment volume described in section 3.5 by the TIN surface area of the
395 study reach. Because floodplain fine sediment depth among study reaches was significantly
396 different between confined and unconfined reaches ($p < 0.05$), we accounted for varying degrees
397 of confinement by standardizing sediment depth by the mean valley width. Using stepwise linear
398 regression, we examined the influence of potential predictor variables (e.g., six-year average
399 number of logjams, drainage area, elevation, stream gradient) on floodplain fine sediment depth.
400
401 *3.7 Analysis of stream and soil water chemistry*
402 Additional surface water and soil samples were collected at the two intensive study sites
403 that captured channel transitions (single thread-multithread-single thread) on Ouzel and Glacier
404 creeks (August 18 and 19, 2014). We used these channel transitions to examine relative changes
405 in dissolved OM composition upstream and downstream of the multithread reaches. The Ouzel
406 Creek intensive study site was ~1,330 m long, with an upstream confined reach of 180 m, and a
407 middle multithread reach of 800 m, and a lower confined reach of 350 m in length. The Glacier
408 Creek intensive study site was ~220 m long, with an upper confined reach of 65 m, a middle
409 multithread reach of 90 m, and a lower partly confined reach 65 m in length. Transects were
410 located near both the upstream and downstream extent of each of the three reaches, which
411 resulted in six transects that defined the two intensive paired sites. Soil core sample locations
412 were selected on both channel banks of each transect and an island within each transect using the
413 same random selection process described in section 3.2. Litter was removed, and fine mineral
414 sediment was sampled where present (some locations were located on bedrock, boulders, or
415 contained only litter) in increments of ~15 cm until refusal at bedrock or gravel. The number of
416 soil samples collected at each site varied by the depth of available fine sediment/mineral soil,

which was sometimes zero (Supplemental Table S3). Surface-water samples were collected at one location along each of the confined transects and within the main stem and from at least one side channel along the multithread reaches (totaling 8 samples for Glacier Creek and 9 samples for Ouzel Creek). Acid-washed Nalgene® HDPE bottles were rinsed six times with water before a sample was collected. All samples were taken back to the lab where soil samples were frozen until further analysis and water samples were processed within six hours.

We quantified dissolved organic carbon (DOC) concentrations in surface-water samples and floodplain soils and fine sediments. Within six hours of collection, samples were filtered through pre-combusted (400°C) 0.7 μm glass fiber filters (Whatman GF/F) and acidified to pH 3. DOC was determined by high-temperature combustion catalytic oxidation using a Shimadzu TOC-V_{CPN} analyzer equipped with a sparging method for non-purgeable OC (hereafter referred to as DOC) (Shimadzu Corporation Columbia, MD). Detection limits for DOC was 50 μg L^{-1}. Five grams of floodplain soil and 10 mL of nanopure water (< 18.2 MΩ-cm) were weighed into sterile 50 mL centrifuge tubes fit with 0.45 μm spin filters. Samples were then centrifuged for 20 minutes at 3,400 rpm and 24°C.

We assessed the structural properties (related to DOM source and bioavailability) of UV-fluorescent dissolved organic matter (FDOM) in surface-water and floodplain soil water leachates using an Aqualog spectrofluorometer equipped with a xenon excitation source (Horiba-Jobin Yvone Scientific Edison, NJ). Filtered surface- and floodplain-water extracts were normalized to 5 mg-C $L^{-1,}$ to reduce inner-filter effects. Excitation emission matrices (EEMs) fluorescence scans were completed from 240-nm to 600-nm excitation and emission wavelengths, with 3-nm band-pass, 3-nm increments, and 3-second integrations. A sealed cuvette of deionized (DI) water was analyzed between every 10 samples to account for

instrument drift and minimize the influence of water Raman peaks in sample spectra. Scans were blank corrected using DI water and corrected for inner filter effects (Kubista et al. 1994). First and second order Raleigh scattering were masked (10-nm width masking), and samples were normalized by the area of the DI water Raman scattering peak (Lawaetz and Stedmon, 2009).

We quantified five spectral FDOM regions to assess the complexity and heterogeneity of surface-water and floodplain soil water leachates using the fluorescence regional integration (FRI) approach (Matlab R2016b) as outlined by Chen et al. (2003). EEMS regions I and II are related to simple proteins (with similar fluorescence characteristics as tyrosine and tryptophan). Region III is related to lower molecular weight, aromatic compounds similar to fulvic acids. Region IV resembles soluble microbial byproducts, and region V is linked with polyaromatic compounds similar to lignin derivatives, tannins, and polyphenols (Chen et al., 2003; Fellman et al., 2010). As the FRI approach quantifies regions of wavelength-dependent fluorescent intensities, it is well suited to capture the underlying heterogeneity and compositional quality of DOM leached from floodplain soils (Chen et al., 2003; Lynch, et al., 2019). Ultraviolet absorbance at the 25 nm wavelength was divided by DOC concentration to calculate $SUVA_{254}$ (L mg C^{-1} m^{-1}), an indicator of fluorescing dissolved organic matter (FDOM) aromaticity or complexity (Weishaar et al., 2003).

3.8 Tracer application and measurements of discharge

Salt tracer applications were used to estimate stream discharge at each intensive study site on the day of sampling for surface water and soils used in fluorescence analysis (see section 3.7). After surface water and soil sample collection was completed, stream tracer additions of NaCl were added as a single pulse to the upstream end of the upper confined study reach for

Ouzel Creek (10,000 g) and Glacier Creek (6000 g) intensive study sites. Downstream changes in specific conductivity were monitored (3-s logging interval, Hobo Conductivity Logger; Onset, Bourne, Massachusetts) at the downstream end of the upper confined reach. Conductivity sensors were removed after conductivity reached background conditions. The total specific conductivity from the tracer application was calculated by integrating beneath the specific conductivity curve. The tracer applications were used to calculate discharge (Q) flowing into at each of the two intensive study sites as

$$Q = \frac{SC_{added}}{\sum_{i=1}^{n}(SC_{meas}\, x\, \Delta t)} \quad \text{(Eq. 1)}$$

where SC_{added} was the specific conductivity of the NaCl added at the upstream end of each intensive study site, and Δt was the duration of each time step (3 s). SC_{meas} was the specific conductivity measured at the downstream end of each reach and corrected for ambient conductivity. NaCl tracer additions were conducted as part of an unpublished NaNO3 uptake study. Additional details and appropriate corrections associated with these salt applications are provided in *Supporting Information*.

3.9 Statistical Analysis

Statistical analyses included examination of correlations, pairwise comparisons, transformations, and stepwise linear regression, which were all conducted using R statistical software (R Core Team, 2017).

Differences in OC storage per area within wood, sediment, and litter (and the sum of all three reservoirs) between valley types was tested using Tukey HSD pairwise comparisons. For these comparisons, storage in large wood, soil OC, and the sum of all three reservoirs required

log transformation to meet assumptions of normality and homoscedasticity; OC storage in litter required no transformation.

We reduced variable redundancy in regression analyses by eliminating independent variables that were strongly cross-correlated, or inherently linked, with other variables (Supplemental Tables S4, S5). To examine factors that controlled OC storage per area and the depth of floodplain fine sediment, potential predictor variables were selected using the following systematic process: the predictor most strongly correlated with the outcome variable was selected as the first predictor and all other variables highly correlated ($r > 7$) with any previously selected variables were eliminated.

Once variable selection was completed, exhaustive (backward and forward) stepwise multiple linear regression was conducted to determine the model that best explained the outcome variable as indicated by the minimized Akaike Information Criterion (AIC; Akaike, 1998). OC storage per area was transformed with a boxcox power transformation (to meet the assumptions of normality and homoscedasticity) to identify variables that influenced the combined OC storage in all three reservoirs (i.e., wood, sediment, litter). No transformations were needed to meet regression assumptions when predicting fine sediment depth normalized by valley width (stepwise linear regression metrics, transformations, and results are listed in Table 3). We evaluated normality of model residuals with Shapiro-Wilk tests (*shapiro.test* in R) and examination of qq-plots and histograms. Homoscedasticity was verified by failing to reject the null hypothesis with an alpha level of 0.05 for the studentized Breusch-Pegan test (*bptest* function in R).

Principle components analysis (PCA) was conducted on EEMS indices to examine differences in the chemical composition of OC in surface waters and floodplain leachates collected along intensive single thread-multithread-single thread reaches.

4. RESULTS

We find that OC storage is greatest in regions with deep floodplain sediments, particularly within unconfined single thread channels and our results indicate logjams play a substantial role in reducing OC in multithread stream reaches. The strongest predictors of sediment depth included channel slope, valley confinement, and the number of logjams (6-year average). Relative to unconfined single thread channels, multithread stream reaches had shallower sediments, lower mean OC contents, and evidence of increased microbial activity and OM transformation.

The following subsections summarize OC storage per area in the three reservoirs (wood, sediment, and litter), focusing on (1) differences in OC storage by valley and channel type (24 study reaches), (2) the role of logjams and channel geometry on floodplain sediment depth (subset of 9 study reaches), and (3) downstream shifts in FDOM composition through transitions in channel complexity in logjam-induced multithread reaches (2 intensive study sites).

4.1 Organic carbon storage by valley type in wood, litter, and sediment

Floodplain OC storage in the study area was dominated by the fine sediment component (102 ±35 to 464 ±165 Mg C ha^{-1}) for all channel types, but relative amounts of storage in all reservoirs differed across valley and channel type (Figure 2). Unconfined single-thread reaches stored more OC in fine sediment (464 ±165 Mg C ha^{-1}) than beaver meadows (276 ±179 Mg C ha^{-1}) and significantly more than confined and partly confined reaches (Table S6). Among all the study reaches, large floodplain wood loads (13 ±23 to 42 ±3 Mg C ha^{-1}) were the smallest

reservoir for OC storage (Table S6), followed closely by litter (20 ±12 to 40 ±7 Mg C ha^{-1}). Among all channel types, beaver meadows contained the lowest OC storage as large floodplain wood and litter (13 ±23 Mg C ha^{-1}) and multithread channels stored the most (42 ±3 Mg C ha^{-1}). Higher OC storage in wood and litter within multithread reaches, relative to beaver meadows and unconfined single thread streams, reflects the abundance of old growth conifer trees in multithread reaches and the limited number of trees in grass- and willow-dominated meadows.

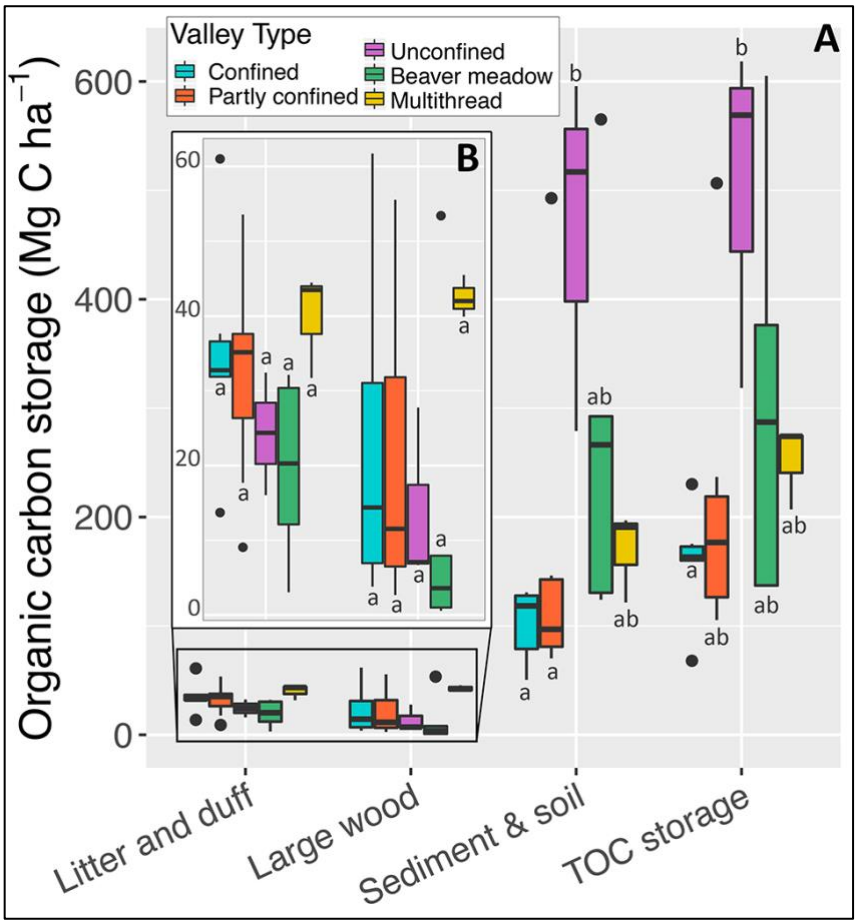

Figure 2. Bar plots of OC storage per area. 24 study reaches are represented by five valley types that vary by degree of confinement and channel complexity. (A) TOC (total OC) is the sum of combined OC stored in (i) litter, (ii) large wood, and (iii) floodplain fine sediment and soil. (B) The zoomed in area of OC storage as wood and litter using a different scale provides details of differences between channel type. Letters a and b indicate group assignments for channel types within each OC reservoir (based on statistical significance at the 95% confidence level using Tukey HSD pairwise comparisons). Channel types sharing any combination of a or b are not significantly different, whereas channel types that do not share a common letter are significantly different.

Unconfined valleys (confined, beaver meadow, and multithread reaches) stored more OC (346 ±177 Mg C ha^{-1}) per area in all reservoirs compared to more narrow valleys (confined and partly confined reaches; 188 ±107 Mg C ha^{-1}) (Figure 2, Table S6). Unconfined single-thread reaches stored significantly more OC in all combined reservoirs than confined reaches (Figure 2). Within unconfined valleys, OC storage differed across reach type depending on channel complexity (i.e., beaver meadows, multithread, unconfined single thread reaches). Single-thread channels (502 ±161 Mg C ha^{-1}) stored more OC per area than more complex beaver meadows (309 ±195 Mg C ha^{-1}) and multithread reaches (252 ±39 Mg C ha^{-1}) (Figure 2, Table 2).

Table 2

Floodplain organic carbon storage in litter, large wood, and soil + fine sediment among all study reaches.

			Wood		Litter and humus		Soil and sediment				Combined
Stream	Valley type	Valley area (ha)	Volume (m^3)	Carbon storage (Mg C ha^{-1})	Volume (m^3)	Carbon storage (Mg C ha^{-1})	Mean SOC (%)	Mean depth (m)	Volume (m^3)	Carbon storage (Mg C ha^{-1})	Carbon storage (Mg C ha^{-1})
NSV	Confined	0.09	16.8	36.5	82.4	61.0	3.0	0.25	229.8	67.7	165.3
Ouzel	Confined	0.02	6.6	61.7	19.3	37.6	6.6	0.22	47.3	130.8	230.1
Glacier	Confined	0.01	0.6	14.1	7.3	33.5	14.4	0.09	7.9	112.3	159.8
NSV	Confined	0.03	2.1	14.7	26.1	31.8	9.7	0.15	41.4	128.8	175.3
NSV	Confined	0.04	0.8	3.8	18.0	13.7	2.6	0.21	90.3	50.5	68.0
Glacier	Confined	0.04	0.9	4.6	27.6	32.0	8.7	0.16	59.4	124.5	161.1
NSV	Partly confined	0.30	17.5	11.5	209.9	37.7	4.4	0.19	590.0	76.7	126.0
Ouzel	Partly confined	0.06	15.8	55.5	47.4	35.0	9.2	0.18	100.6	146.3	236.8
Glacier	Partly confined	0.26	28.2	21.4	200.3	35.1	4.0	0.19	509.2	70.2	126.7
Hunters	Partly confined	0.05	10.7	42.2	40.0	37.5	3.2	0.33	169.1	96.9	176.7
NSVNSV	Partly confined	0.26	3.5	2.7	51.8	17.7	3.0	0.32	815.6	85.0	105.4
Glacier	Partly confined	0.05	1.1	4.7	14.4	9.1	13.2	0.42	193.0	492.8	506.6
NSV	Partly confined	0.43	17.7	8.3	299.6	53.6	3.4	0.46	1966.3	139.0	200.8
Cony	Unconfined	0.13	18.4	27.8	47.1	24.4	19.0	0.30	402.4	516.9	569.1
Glacier	Unconfined	0.15	5.0	6.7	80.1	16.0	13.5	0.49	729.5	595.7	618.5
Mills	Unconfined	0.21	7.4	7.1	173.6	32.4	5.4	0.57	1186.3	279.1	318.6
NSV	Beaver	0.58	23.0	7.9	546.1	32.1	11.6	0.54	3126.2	565.1	605.2
Ouzel	Beaver	0.30	79.5	53.4	265.5	30.4	12.5	0.26	773.7	292.5	376.3
NSV	Beaver	5.04	14.7	0.6	2109.6	20.3	5.2	0.57	28798.5	266.3	287.2
BTR	Beaver	3.27	16.4	1.0	1090.6	12.1	2.3	0.60	19501.1	124.0	137.2
SFP	Beaver	0.81	14.6	3.6	91.5	3.1	2.8	0.51	4187.5	130.4	137.1
NSV	Multithread	0.49	103.1	42.0	558.5	43.5	5.2	0.26	1269.3	121.5	207.0
Glacier	Multithread	0.12	26.8	45.5	106.0	31.7	9.6	0.23	268.6	196.9	274.1
Ouzel	Multithread	0.37	74.1	39.9	452.4	44.5	8.9	0.24	881.7	190.7	275.1

Note: Reach abbreviations include BTR = Big Thompson River, GCK = Glacier Creek, NSV = North Saint Vrain Creek, SFP = South Fork Cache La Poudre River

Stepwise regression results indicate that OC storage per area is greatest in less confined valleys, low-gradient streams, and at higher elevations. The optimal regression model explaining potential controls on the amount of OC storage per area includes elevation, stream gradient, and valley confinement (Table 3). This makes sense because narrow valley types (confined and partly confined reaches) that store less OC per area have steeper stream gradients and are more confined. Valley confinement also increases below the terminal extent of Pleistocene glaciation and the knickpoint at the contact between igneous and sedimentary rocks. Unconfined single thread and beaver meadow reaches are less confined and tend to have lower stream gradients than multithread reaches and narrower valley types (Table 1).

Table 3 Stepwise regression transformations and results

	Combined OC storage		Fine sediment depth standardized by valley width	
Transformation	λ = -0.38384		n/a	
Intercept	3.49E-01	***	-9.11E-02	
Elevation	-8.17E-05	***	3.53E-05	
Stream gradient	3.34E-01	*	1.60E-01	*
Confinement	-1.11E-03		n/a	
Drainage area	n/a		-6.77E-04	
Annual average number of logjams	n/a		-2.40E-03	*
r2	0.7093	***	0.7374	*
p-value	3.46E-06		0.05	

*Note: statistical significance for each variable and optimal multiple linear regression model denoted with *** for p<0.001, ** for p<0.01, * p<0.05, and . for p<0.1*

	Combined OC storage	Fine sediment depth standardized by valley width
Transformation	λ = -0.38384	n/a

Intercept	3.49E-01	***	-9.11E-02	
Elevation	-8.17E-05	***	3.53E-05	
Stream gradient	3.34E-01	*	1.60E-01	*
Confinement	-1.11E-03		n/a	
Drainage area	n/a		-6.77E-04	
Annual average number of logjams	n/a		-2.40E-03	*
r^2	0.7093	***	0.7374	*
p-value	3.46E-06		0.05	

*Note: statistical significance for each variable and optimal multiple linear regression model denoted with *** for p<0.001, ** for p<0.01, * p<0.05, and . for p<0.1*

566 Differences in OC storage among the three unconfined valley types (beaver meadows,
567 multithread, and unconfined single thread reaches) are reflected in sediment depth and OC
568 content. Beaver meadows and unconfined single-thread channels have higher mean floodplain
569 fine sediment depth than multithread channel reaches, although these differences are not
570 statistically significant (Figure 3A). Unconfined single-thread study reaches also have the
571 highest mean OC content across all channel types and substantially more than multithread
572 channel reaches (Figure 3B).
573

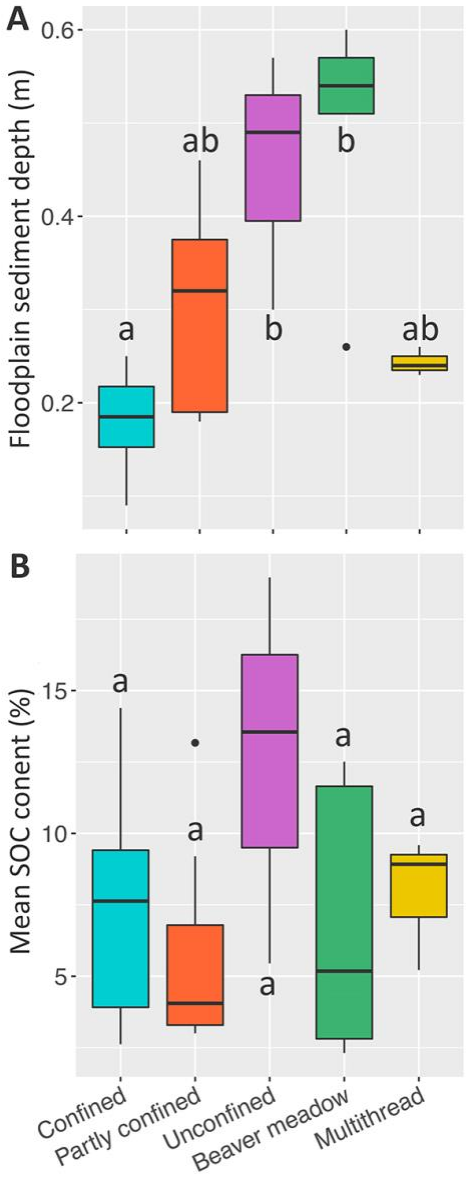

Figure 3. Boxplots of floodplain soil depth and mean soil organic carbon content (OC) by valley type. Letters *a* and *b* indicate group assignments for channel types within each OC reservoir (based on statistical significance at the 95% confidence level using Tukey HSD pairwise comparisons). Channel types sharing any combination of a or b are not significantly different, whereas channel types that do not share a common letter are significantly different.

4.2 Logjams and fine sediment storage

The optimal model from stepwise multiple linear regression indicates that ~74% of the variability in average floodplain fine sediment depths, standardized by valley width, is best explained by the six-year average number of logjams, stream gradient, drainage area, and

585 elevation (Table 3). This means that increased number and frequency of logjams within a given
586 river segment is linked with shallower floodplain fine sediment when also considering valley
587 width and stream gradient (Supplemental Table S5).

588 ***4.3 Organic matter composition in multithread intensive study reaches***

589 Using principal components analysis (PCA), we identified relationships between channel
590 complexity and the structural characteristics of fluorescing dissolved OM (FDOM) collected
591 from stream flow and adjacent floodplain soils within the two intensive study segments.

592 FDOM signatures of stream water samples indicate distinct changes in DOM
593 composition at transitions from confined to multithread channels that influence the downstream-
594 most reach within the intensive study sites. Stream water (Figure 4A) flowing from confined
595 reaches into multithread channel reaches had optical properties consistent with terrestrially
596 derived organic acids (regions III and V). FDOM complexity ($SUVA_{254}$) and the relative
597 abundance of protein-like compounds (EEMS regions I, II) that are typically associated with
598 microbial sources (Lynch, et al., 2019) increased within multithread networks. Regions II and V
599 were also more variable within multithread reaches, potentially reflecting more diverse pathways
600 for microbial transformation of terrestrially-derived OC. Surface water flowing through lower
601 confined reaches retained the heterogeneous signature imparted by multithread channels, with
602 relatively more microbially-derived proteinaceous features than upper confined reaches (Figure
603 4C).

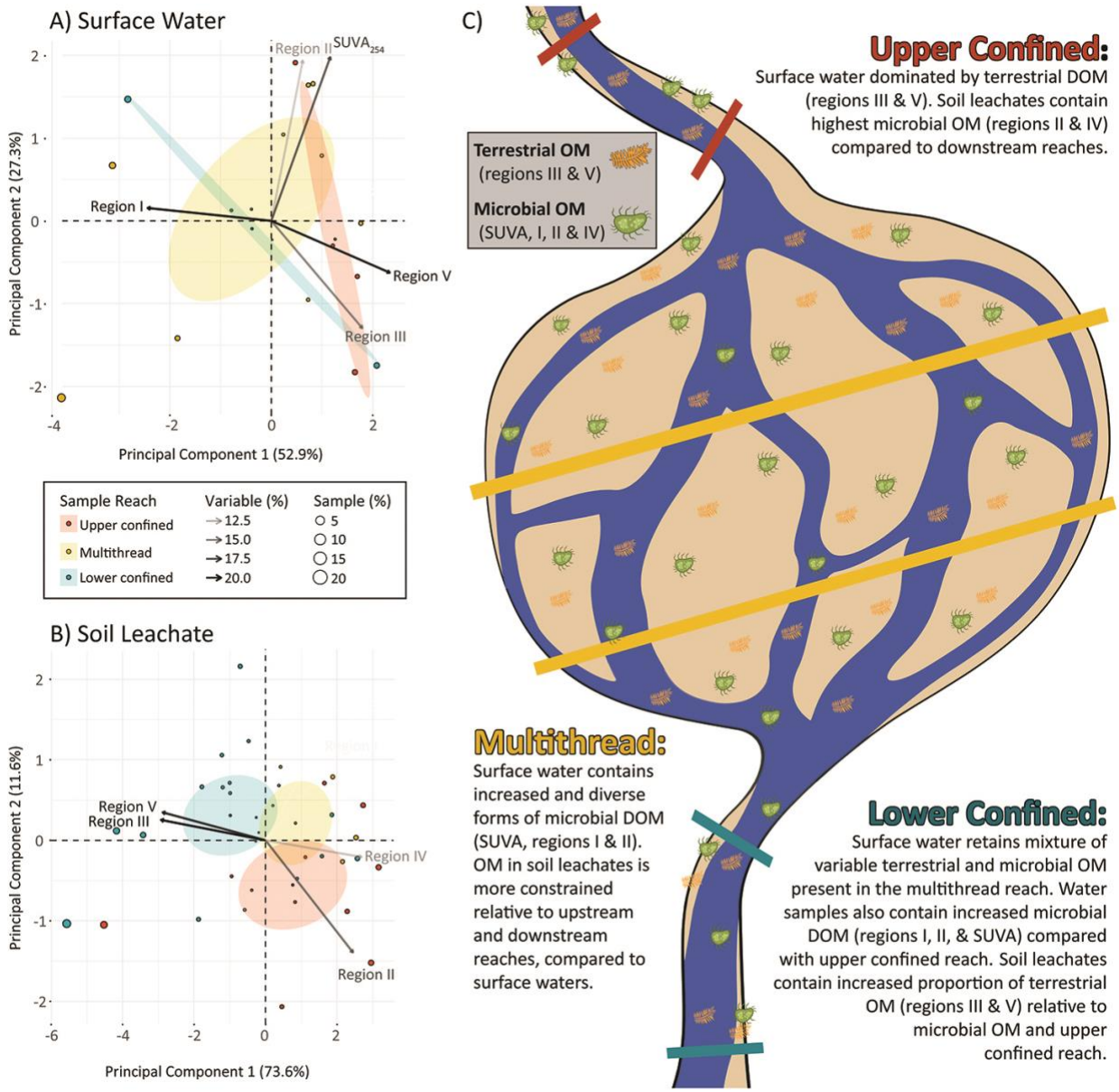

Figure 4. Principal components analysis (PCA) of FDOM composition (A, B) and a diagram illustrating results as a function of channel complexity (C). The contribution (in percent) of individual variables (vector shade) and samples (symbol size) to principal components 1 and 2 are shown for (A) surface waters and (B) soil leachates (data provided in Table S7). Shaded ellipses correspond to 95% confidence intervals for the upper confined (red), lower confined (blue), and middle multithread (yellow) reaches. The diagram (C) depicts two sampling transects within each reach (colors match PCA plots).

EEMS spectra of floodplain soil leachate contained a similar, but opposite, shift in the signatures of DOM at the study sites. The relative intensities of EEMS regions II and IV (representing simple proteins and byproducts of microbial metabolism) were highest in soil

leachate collected from upper, confined reaches flowing into multithread channels (Figure 4B). Similar to the pattern found in surface waters, the fluorescent properties of floodplain soil leachates within multithread reaches reflect both terrestrial and microbial-derived OC. However, the variability in fluorescence spectra of floodplain leachates collected from multithread reaches was more constrained, relative to upstream and downstream single-thread reaches, than that found in adjacent surface waters (Figure 4B). Floodplain soil leachates collected from lower, confined reaches had higher relative percent intensities of regions III and V, reflecting a more diverse array of terrestrially-derived organic acids relative to the upstream reach.

In both surface waters and floodplain soil leachates, FDOM variability was highest in multithread reaches. Although FDOM variability decreases in single-thread planform downstream of multithread reaches, some complexity of FDOM within multithread reaches is retained within lower single-thread reaches relative to upper confined channels (Figure 4C).

Discharge during the time of sampling was typical of mean flows in August at the base of receding limbs of annual snowmelt-dominated hydrographs. Discharge measured from tracer additions at the intensive study sites were 0.27 $m^3 s^{-1}$ at Ouzel Creek and 0.20 $m^3 s^{-1}$ at Glacier Creek. We use relative comparison of discharge during typical years and the time of sampling at a USGS gauge ~8 km downstream from the Glacier study site to place our measured discharge values into context. Monthly average discharge at the Big Thompson Creek gauge at Moraine Park during June, July, August, and September are 7.37, 3.64, 1.38, and 0.86 $m^3 s^{-1}$. For comparison, discharge at the Big Thompson River gauge downstream of the Glacier Creek intensive study site was 1.39 $m^3 s^{-1}$ during the day of sampling for fluorescence on 19 August, 2014 (Figure S2).

5. Discussion

5.1 Organic carbon storage by valley type and valley-channel morphology

Our findings build upon previous work by showing that unconfined valleys store more OC per area than confined valleys (Wohl et al., 2012), but also elucidate mechanisms to explain why OC storage per area is not highest in logjam-induced multithread channels. While OC storage in beaver meadows was not as high as unconfined single-thread channels, they do constitute substantial storage. Other studies report similar levels of OC storage in Colorado Front Range (CFR) beaver meadows, but suggest OC storage decreases when meadows are abandoned (Wohl, 2013; Laurel & Wohl, 2019). Following beaver abandonment, channels incise and water tables decline, which likely cause decreased fluvial deposition of OM across the floodplain and loss of riparian vegetation. Seasonal changes in hydrologic connectivity have also been correlated with shifts in the molecular composition of OM flowing through multithread beaver meadows (Lynch, et al. 2019). During base-flow conditions, Lynch et al. (2019) found that hydrologic connectivity declined and DOM diversity increased. The authors contributed these observations to hydrologic fragmentation and greater turnover and release of microbial metabolites. The results we present here suggest similar hydrologic controls catalyze OM transformation, because fine-sediment OC content is lower in multithread channel reaches and FDOM signatures indicate an increase microbial transformation of OM in these complex streams.

Lower OC storage in the floodplain sediments of multithread channels is driven by two primary characteristics among the study reaches: (1) shallower fine sediments and (2) lower OC content. Our results inform two conceptual models described in detail below that explain observed decreases in fine sediment depth and OC content along multithread reaches.

662

663 *5.2 Logjams and floodplain fine sediment depth*

664 The mean depth of floodplain fine sediment along single-thread channels in unconfined
665 valleys (45 ± 14 cm) is deeper (although not significantly, $p = 0.3$) than multithread channels (24
666 ± 2 cm; Figure 3.). As a result, fine sediment volume and OC storage per area is higher in
667 unconfined single-thread than multithread reaches despite similar valley widths.

668 Recruitment of old-growth trees into the stream channel and the formation of channel-
669 spanning logjams can facilitate floodplain aggradation and complex topography in headwater
670 streams (Sear et al., 2010), stabilizing vegetated islands and fine sediment storage in large
671 alluvial valleys (Collins et al., 2012). However, our results along smaller streams (< 200 km^2),
672 suggest multiple channels of flow across the valley bottom limit total fine sediment storage for
673 valleys of similar width.

674 Large instream wood and logjams act in tandem to separate flow, decreasing flow depth
675 and shear stress. Because large wood and logjams obstruct flow in channels, they dissipate force
676 acting on the bed and partition shear stress so that less shear stress is available to transport
677 sediment (Manga & Kirchner, 2000). The accumulation of gravels behind logjams (Cadol &
678 Wohl, 2011), further divert flow into multiple channels. Limited competence to mobilize coarser
679 sediment could in turn facilitate bank erosion, undercutting of trees, and channel avulsions (Sear
680 et al., 2010; Polvi & Wohl, 2013). Transport of fine sediment within multithread reaches across
681 the relatively low floodplain further limits fine sediment aggradation across the floodplain and
682 vegetated bars (see Extended Discussion in Supplemental Material).

683 In contrast, single-thread unconfined channel floodplains dominated by densely growing
684 rushes, sedges, and woody shrubs stabilize channel banks and provide erosion resistance (Simon

& Collison, 2002). Energy dissipation across the broad floodplains of single-thread channels results in fine overbank sediment accumulation, providing additional bank cohesion and erosion resistance. Transport of both fine and coarse sediment in the channel and aggradation of the floodplain increases channel cross sectional area and the ability to convey larger flows. The resulting increase in potential bed shear stress ensures continued transport of coarse grains and a positive feedback that maintains a single-thread channel. Accumulation of floodplain fine sediment and release of OM from floodplain vegetation (litter and root exudate inputs) may further increase OC storage per area in single thread channels of unconfined valleys.

5.3 Multithread channels as hotspots for OM transformation

Multithread reaches contain lower OC content in floodplain fine sediments than their single-thread counterparts flowing through unconfined valleys (Table 2). This result is linked to two primary factors: (1) differences in OC sources and (2) inferred differences in mixing and the transit time of water and entrained OC in multithread and unconfined single thread reaches.

Although we assume a substantial portion of OC inputs to floodplains in the CFR are fluvially transported, a portion of OC is derived from *in-situ* sources of OC, which differ between logjam-induced multithread reaches and unconfined valley segments. Within our study sites, multithread reaches lack abundant vegetative ground cover. Our observations of the highest wood and litter storage in multithread channel compared with other stream types indicate that coarse particulate OM is a substantial source of floodplain OC in multithread channels . In contrast, unconfined single-thread reaches have abundant rush and sedge communities, which likely release root exudates and litter directly to the floodplain. Thus, differences in riparian

vegetation, which co-vary with channel morphology, likely play a role in OC storage by influencing OM inputs and quality (i.e., potential decomposability).

Higher moisture content observed on the floodplain surface of unconfined single-thread floodplains compared to multithread reaches likely facilitates positive feedbacks with bedrock chemical weathering. Increased moisture at the bedrock/regolith interface increases chemical weathering and bedrock fracturing, which in turn could increase groundwater input into these reaches. Groundwater discharge could facilitate increased OC concentrations along unconfined floodplains, but organic-rich sedimentary rocks are virtually non-existent in the study area (Braddock & Cole, 1990). At the same time, high soil moisture within old growth forest floodplains may limit (1) conifer growth, (2) wood recruitment to channels, (3) logjams, and (4) the transition into multithread channel systems, creating a stable state for moist, grassy floodplains with few conifers.

Our observations of downstream shifts in FDOM composition within the Glacier and Ouzel Creek intensive study sites provide mechanistic insight into the influence of channel complexity on organic carbon storage (Figure 4C). We observed that flow in single-thread channels upstream of multithread systems had a higher relative abundance of FDOM compounds characteristic of terrestrial inputs (Figure 4A). In contrast, upstream single-thread floodplain leachates reflected the signatures of microbial activity working to break down that OM (Figure 4B). Greater structural heterogeneity within the FDOM pool and higher relative abundance of protein-rich microbial derivatives are present in multithread channels. FDOM signatures in downstream narrow single thread channels reflect fluvial transport of complex terrestrial DOM from upstream multithread reaches. This lingering increase in FDOM complexity suggests

abundant hyporheic exchange, increased microbial transformation of OM, and OM flushing from floodplain sediment within multithread channel reaches.

Our findings reflect increased opportunities for terrestrial-derived OM (e.g. lignin-derivatives and higher molecular weight organic acids) to be compositionally altered by microbial transformation or photo-oxidation through abundant mixing and hyporheic exchange in multithread channels. Channel complexity promotes increased hyporheic exchange, oxygen availability, and water and DOC transit times (Danczak et al., 2016; Gooseff et al., 2007). These conditions in complex channels facilitate oxidation of OM (Battin et al., 2008; Boye et al., 2017), flushing of OM from floodplain sediment, and mixing of OM pools in both sediment and surface waters (Stegen et al., 2016; Figure 4C). Thus, microbial and invertebrate communities have greater opportunities to assimilate and transform OM, reducing OC storage through CO_2 mineralization to the atmosphere. These transformations have important implications for substrate quality as FDOM is exported to higher-order river networks.

Findings presented here support past work that identified morphologically complex multithread streams as hotspots for the decomposition and transformation of OC (Battin et al., 2008; Lynch, et al., 2019). These complex channels in the CFR support higher aquatic invertebrate, rainbow trout, and cutthroat trout biomass relative to less-complex, single-thread channels (Livers & Wohl, 2016; Wohl et al., 2017; Herdrich et al., 2018; Venarsky et al., 2018). Here we show that increases in microbial activity and OM turnover within complex multithread reaches may provide the resources necessary at the bottom of the food web to facilitate increased productivity in these mountainous stream ecosystems.

6 Implications: *Floodplain organic carbon dynamics under shifting hydrologic regimes*

751 Incorporating floodplain C dynamics into the terrestrial OC budget requires investigating
752 potential changes in hydrologic flow regime, floodplain hydrologic connectivity, erosion, and
753 sedimentation that could alter sediment and OC floodplain reservoirs. The dynamic nature of
754 rivers and their sensitivity to anticipated changes in precipitation and hydrologic flow regimes
755 are poised to trigger changes in sediment dynamics and hydrologic connectivity that may shift
756 the role of floodplains as OC sinks or sources (Sutfin et al., 2016). Observed decreases in
757 snowpack and earlier snowmelt (Stewart, 2009), elevational shifts in rain-snow transitions
758 (Kampf & Lefsky, 2016), and changes in precipitation regimes may drastically alter the timing,
759 frequency, and magnitude of river flows (Bates et al., 2008).
760 Observed and projected changes in river flows in response to land use and flow
761 regulation are well known (Dunne & Leopold, 1978; Richter et al., 1996; Poff et al., 1997), but
762 those associated with climate change are riddled with uncertainty (Hirsch & Archfield, 2015;
763 Sharma et al., 2018; Gudmundsson et al., 2019; Tabari, 2020). Possible responses to a changing
764 climate could result in different changes in floodplain OC storage within the CFR and similar
765 snowmelt-dominated mountainous systems, particularly under additional societal pressure of
766 land use and flow regulation. We consider two possible contrasting, but not mutually exclusive,
767 hydrologic responses (increase in floods and the loss of hydrologic connectivity) under a
768 changing climate and societal pressure. Our results suggest OC storage in floodplains will
769 respond to these changes differently depending on channel and valley geometry.
770 Extreme precipitation may increase the magnitude of rare extreme floods (Gudmundsson
771 et al., 2019; Tabari, 2020) – which are exacerbated by deforestation (Dunne & Leopold, 1978),
772 urbanization (Blum et al., 2020), and wildfire (Moody & Ebel, 2012) – and alter floodplain
773 aggradation, erosion, and OC storage. Steeper river channels in confined valleys in the CFR

774 Montane zone are particularly susceptible to large floods (Sutfin & Wohl, 2019). Losses in
775 floodplain sediment and associated OC storage were observed following the 2013 flood in the
776 CFR (Rathburn et al., 2017), which evacuated floodplain fine sediment after sample collection
777 occurred at four of our study reaches.

778 In contrast, wider valleys have the capacity to accommodate floods, dissipate flow
779 energy, and attenuate flood waves, all of which facilitate increases in aggradation of fine
780 sediment (Dunne & Leopold, 1978; Wohl et al., 2015) and OC storage. Our observations indicate
781 deeper fine sediment and higher OC content in unconfined single thread reaches. Because high-
782 elevation, unconfined valleys that are unaltered by wildfire in the last 500 years store sediment
783 for greater than 1,200 years in the study area (N. A. Sutfin & Wohl, 2019), we can assume
784 contemporary floodplain sediment represents accumulation and storage over a range of annual
785 floods up to the approximate 1000-year flood. This indicates that single thread and multithread
786 streams in unconfined valleys will facilitate increases in sediment and OC storage during floods
787 under both projected increases in extreme events (Gudmundsson et al., 2019; Tabari, 2020) and
788 observed increases in the frequency of smaller floods (Hirsch & Archfield, 2015; Sharma et al.,
789 2018). These changes in flood frequency and magnitude are likely to influence OC accumulation
790 depending on valley geometry, but our results indicate that channel complexity will regulate the
791 mineralization of and decrease in stored OC.

792 Anticipated decreases in hydrologic connectivity across valley bottoms in response to
793 decreased snowpack, more frequent drought, or lower baseflows (Stewart, 2009; Alexander et
794 al., 2015) will affect OC storage in unconfined valleys depending on channel complexity.
795 Decreases in lateral connectivity across valley bottoms limit overbank floodplain deposition,
796 which could limit OC storage in unconfined single thread valleys. However, we anticipate a

more complex response in multithread channel reaches, in which our results indicate increased microbial activity and transformation of OM. Projected decreases in lateral and longitudinal hydrologic connectivity under a changing climate, flow diversions, and dams will decrease local ground water table elevations and rates of hyporheic exchange (Alexander et al., 2015). Because seasonal decrease in connectivity has been linked to increased microbial transformation of OM in complex multithread streams (Lynch, et al., 2019), our observed increase in FDOM diversity in multithread reaches of our study sites are indicative of the relatively low flow conditions during the time of sampling. Thus a loss of connectivity in reaches that already exhibit lower OC content and higher microbial mineralization of OM, could facilitate a significant loss in OC storage and sources of OM to downstream food webs.

7 Conclusion

Mountainous headwater streams are important components of the terrestrial carbon cycle, contributing to long-term carbon storage and ecosystem productivity. Stepwise regression results presented here indicate that OC storage along river corridors of the CFR is higher in relatively unconfined valleys, in low-gradient valleys, and at higher elevations. Our results show that unconfined valleys store more OC per area than more confined valleys, but single thread channels store more OC than more complex multithread channels in unconfined valleys. We attribute this in part, to the dissipation of energy along elevated, cohesive, and grass-dominated floodplains of single thread channels in unconfined valleys that promote the aggradation of fine sediment and OC. However, the aggradation of floodplain fine sediment and OC storage is limited where channels in unconfined valleys develop multithread channel planforms in response to persistent channel-spanning logjams. We posit that decreased flow depth and partitioning of shear stress across logjams and numerous channels of flow in multithread streams limit coarse

sediment transport and facilitate selective transport of finer sediment and OM. These processes limit fine sediment aggradation and the magnitude of OC storage per unit area. Shallower fine sediment storage and increased microbial transformation of OM compared to single thread reaches decrease OC storage. Our results of increased OM transformation and lower OC content in multithread streams compared to single thread channels support observations by others that link channel complexity with increased hyporheic exchange, transit time of water, and opportunities for microbial transformation of OM. Although multithread channels do not store the most OC per area, they serve as hotspots for OM transformation and sources for downstream aquatic food webs. These results suggest that valley geometry and channel complexity regulate the OC-storage response to observed increases in flood frequency, predicted increases in flood magnitude, and anticipated losses in hydrologic connectivity within streams.

Acknowledgements and data availability statement

This paper is based upon work supported by National Science Foundation Grant No. DGE-0966346 "I-WATER: Integrated Water, Atmosphere, Ecosystems Education and Research Program" at Colorado State University (CSU); NSF Doctoral Research Dissertation Improvement Grant #1536186; and graduate student research grants from the Geological Society of America, the Colorado Scientific Society, and the Colorado State University Warner College of Natural Resources and Department of Geosciences. We thank Rocky Mountain National Park their support and research permits, Teagan Deeney and Jim Self at the CSU Soil and Water Laboratory, Mark Pascke for use of his lab, Thomas Borch for his insight and guidance, and assistance in the field and the laboratory by Ben Von Thaden, Dean Anderson, John Harris, Matheus Cruz Lima Pereira, Bryce Johnson, Julia Makiejus, Pamela Wagener, Jon Garber, Joel

Sholtes, and Fernando Javier Ugalde Pascual. All data generated in this study can be accessed through the associated Supporting Information file, http://hdl.handle.net/10217/173334, and Sutfin (2020) cited below.

References

Akaike, H. (1998). A New Look at the Statistical Model Identification. In E. Parzen, K. Tanabe, & G. Kitagawa (Eds.), *Selected Papers of Hirotugu Akaike* (pp. 215–222). New York, NY: Springer New York. https://doi.org/10.1007/978-1-4612-1694-0_16

Alexander, L., Autrey, B., DeMeester, J., & Fritz, K. M. (2015). *Connectivity of Streams and Wetlands to Downstream Waters: A Review and Synthesis of the Scientific Evidence* (Reports & Assessments No. EPA/600/R-14/475F) (p. 408). The U.S. Environmental Protection Agency's (USEPA) Office of Research and Development.

Anderson, R. S., Riihimaki, C. A., Safran, E. B., & MacGregor, K. R. (2006). Facing reality: Late Cenozoic evolution of smooth peaks, glacially ornamented valleys, and deep river gorges of Colorado's Front Range. *SPECIAL PAPERS-GEOLOGICAL SOCIETY OF AMERICA*, *398*(397).

Aufdenkampe, A. K., Mayorga, E., Raymond, P. A., Melack, J. M., Doney, S. C., Alin, S. R., et al. (2011). Riverine coupling of biogeochemical cycles between land, oceans, and atmosphere. *Frontiers in Ecology and the Environment*, *9*(1), 53–60. https://doi.org/10.1890/100014

Ballantyne, A. P., Alden, C. B., Miller, J. B., Tans, P. P., & White, J. W. C. (2012). Increase in observed net carbon dioxide uptake by land and oceans during the past 50 years. *Nature*, *488*(7409), 70–72. https://doi.org/10.1038/nature11299

Barry, R. G. (1973). A Climatological Transect on the East Slope of the Front Range, Colorado. *Arctic and Alpine Research*, *5*(2), 89–110. https://doi.org/10.1080/00040851.1973.12003684

Bates, B., Kundzewicz, Z. W., Wu, S., & Palutikof, J. (2008). *Climate Change and Water. Technical Paper of the Intergovernmental Panel on Climate Change* (Technical Paper VI No. VI) (p. 210). Geneva: IPCC Secretariat. Retrieved from https://digital.library.unt.edu/ark:/67531/metadc11958/m1/13/

Battin, T. J., Kaplan, L. A., Findlay, S., Hopkinson, C. S., Marti, E., Packman, A. I., et al. (2008). Biophysical controls on organic carbon fluxes in fluvial networks. *Nature Geoscience*, *1*(2), 95–100. https://doi.org/10.1038/ngeo101

Beckman, N. D., & Wohl, E. (2014). Carbon storage in mountainous headwater streams: The role of old-growth forest and logjams. *Water Resources Research*, *50*(3), 2376–2393. https://doi.org/10.1002/2013WR014167

Birkeland, P. W., Shroba, R. R., Burns, S. F., Price, A. B., & Tonkin, P. J. (2003). Integrating soils and geomorphology in mountains—an example from the Front Range of Colorado. *Geomorphology*, *55*(1), 329–344. https://doi.org/10.1016/S0169-555X(03)00148-X

Blum, A. G., Ferraro, P. J., Archfield, S. A., & Ryberg, K. R. (2020). Causal Effect of Impervious Cover on Annual Flood Magnitude for the United States. *Geophysical Research Letters*, *47*(5), e2019GL086480. https://doi.org/10.1029/2019GL086480

Boye, K., Noël, V., Tfaily, M. M., Bone, S. E., Williams, K. H., Bargar, J. R., & Fendorf, S. (2017). Thermodynamically controlled preservation of organic carbon in floodplains. *Nature Geoscience*, *10*(6), 415–419. https://doi.org/10.1038/ngeo2940

Braddock, W. A., & Cole, J. C. (1990). Geologic map of Rocky Mountain National Park and vicinity, Colorado. U.S. Geological Survey.

Cadol, D., & Wohl, E. (2011). Coarse sediment movement in the vicinity of a logjam in a neotropical gravel-bed stream. *Geomorphology*, *128*(3), 191–198. https://doi.org/10.1016/j.geomorph.2011.01.007

Chapin, F. S., Matson, P. A., & Vitousek, P. (2011). *Principles of Terrestrial Ecosystem Ecology* (2nd ed.). New York, NY: Springer Science & Business Media.

Chen, W., Westerhoff, P., Leenheer, J. A., & Booksh, K. (2003). Fluorescence excitation - emission matrix regional integration to quantify spectra for dissolved organic matter. *Environmental Science and Technology*, *37*(24), 5701–5710.

Collins, B. D., Montgomery, D. R., Fetherston, K. L., & Abbe, T. B. (2012). The floodplain large-wood cycle hypothesis: A mechanism for the physical and biotic structuring of temperate forested alluvial valleys in the North Pacific coastal ecoregion. *Geomorphology*, *139–140*, 460–470. https://doi.org/10.1016/j.geomorph.2011.11.011

Danczak, R. E., Sawyer, A. H., Williams, K. H., Stegen, J. C., Hobson, C., & Wilkins, M. J. (2016). Seasonal hyporheic dynamics control coupled microbiology and geochemistry in Colorado River sediments. *Journal of Geophysical Research: Biogeosciences*, *121*(12), 2976–2987. https://doi.org/10.1002/2016JG003527

D'Elia, A. H., Liles, G. C., Viers, J. H., & Smart, D. R. (2017). Deep carbon storage potential of buried floodplain soils. *Scientific Reports*, *7*(1), 8181. https://doi.org/10.1038/s41598-017-06494-4

Downing, J. A., Cole, J. J., Duarte, C. M., Middelburg, J. J., Melack, J. M., Prairie, Y. T., et al. (2012). Global abundance and size distribution of streams and rivers. *Inland Waters*, *2*(4), 229–236. https://doi.org/10.5268/IW-2.4.502

Dunne, T., & Leopold, L. B. (1978). *Dunne, Thomas, and Luna B. Leopold. Water in environmental planning*. Macmillan.

Falkowski, P., Scholes, R. J., Boyle, E., Canadell, J., Canfield, D., Elser, J., et al. (2000). The Global Carbon Cycle: A Test of Our Knowledge of Earth as a System. *Science*, *290*(5490), 291–296. https://doi.org/10.1126/science.290.5490.291

913 Fellman, J. B., Hood, E., & Spencer, R. G. M. (2010). Fluorescence spectroscopy opens new windows into
914 dissolved organic matter dynamics in freshwater ecosystems: A review. *Limnology and*
915 *Oceanography*, *55*(6), 2452–2462. https://doi.org/10.4319/lo.2010.55.6.2452
916 FIA. (2019). *Forest Inventory and Analysis National Program - FIA Library*. Washington, D.C.: U.S. Forest
917 Service, FIA Program. Retrieved from https://www.fia.fs.fed.us/library/field-guides-methods-
918 proc/
919 Galy, V., Peucker-Ehrenbrink, B., & Eglinton, T. (2015). Global carbon export from the terrestrial
920 biosphere controlled by erosion. *Nature*, *521*(7551), 204–207.
921 https://doi.org/10.1038/nature14400
922 Glass, S. V., & Zelinka, S. L. (2004). *Wood Handbook Ch 4: Moisture Relations and Physical Properties of*
923 *Wood* (USDA General Technical Report No. FPL-GTR-190) (p. 20). Madison, WI: U.S. Department
924 of Agriculture, Forest Service, Forest Products Laboratory. Retrieved from
925 https://www.fpl.fs.fed.us/documnts/fplgtr/fplgtr190/chapter_04.pdf
926 Gochis, D., Schumacher, R., Friedrich, K., Doesken, N., Kelsch, M., Sun, J., et al. (2014). The Great
927 Colorado Flood of September 2013. *Bulletin of the American Meteorological Society*, *96*(9),
928 1461–1487. https://doi.org/10.1175/BAMS-D-13-00241.1
929 Gooseff, M. N., Hall, R. O., & Tank, J. L. (2007). Relating transient storage to channel complexity in
930 streams of varying land use in Jackson Hole, Wyoming. *Water Resources Research*, *43*(1).
931 https://doi.org/10.1029/2005WR004626
932 Gregory, J. M., Jones, C. D., Cadule, P., & Friedlingstein, P. (2009). Quantifying Carbon Cycle Feedbacks.
933 *Journal of Climate*, *22*(19), 5232–5250. https://doi.org/10.1175/2009JCLI2949.1
934 Gudmundsson, L., Leonard, M., Do, H. X., Westra, S., & Seneviratne, S. I. (2019). Observed Trends in
935 Global Indicators of Mean and Extreme Streamflow. *Geophysical Research Letters*, *46*(2), 756–
936 766. https://doi.org/10.1029/2018GL079725

937 Herdrich, A. T., Winkelman, D. L., Venarsky, M. P., Walters, D. M., & Wohl, E. (2018). The loss of large
938 wood affects rocky mountain trout populations. *Ecology of Freshwater Fish*, *27*(4), 1023–1036.
939 https://doi.org/10.1111/eff.12412
940 Hirsch, R. M., & Archfield, S. A. (2015). Not higher but more often. *Nature Climate Change*, *5*(3), 198–
941 199. https://doi.org/10.1038/nclimate2551
942 Hoffmann, T., Glatzel, S., & Dikau, R. (2009). A carbon storage perspective on alluvial sediment storage
943 in the Rhine catchment. *Geomorphology*, *108*(1–2), 127–137.
944 https://doi.org/10.1016/j.geomorph.2007.11.015
945 Ives, R. L. (1942). The beaver-meadow complex. *Journal of Geomorphology*, *5*(3), 191–203.
946 Jarrett, R. D. (1990). Paleohydrologic techniques used to define the spatial occurrence of floods.
947 *Geomorphology*, *3*(2), 181–195. https://doi.org/10.1016/0169-555X(90)90044-Q
948 Kampf, S. K., & Lefsky, M. A. (2016). Transition of dominant peak flow source from snowmelt to rainfall
949 along the Colorado Front Range: Historical patterns, trends, and lessons from the 2013 Colorado
950 Front Range floods. *Water Resources Research*, *52*(1), 407–422.
951 https://doi.org/10.1002/2015WR017784
952 Laurel, D., & Wohl, E. (2019). The persistence of beaver-induced geomorphic heterogeneity and organic
953 carbon stock in river corridors: Beaver-induced heterogeneity. *Earth Surface Processes and*
954 *Landforms*, *44*(1), 342–353. https://doi.org/10.1002/esp.4486
955 Lininger, K. B., & Wohl, E. (2019). Floodplain dynamics in North American permafrost regions under a
956 warming climate and implications for organic carbon stocks: A review and synthesis. *Earth-*
957 *Science Reviews*, *193*, 24–44. https://doi.org/10.1016/j.earscirev.2019.02.024
958 Livers, B., & Wohl, E. (2015). An evaluation of stream characteristics in glacial versus fluvial process
959 domains in the Colorado Front Range. *Geomorphology*, *231*, 72–82.
960 https://doi.org/10.1016/j.geomorph.2014.12.003

961 Livers, B., & Wohl, E. (2016). Sources and interpretation of channel complexity in forested subalpine
962 streams of the Southern Rocky Mountains: CHANNEL COMPLEXITY IN FORESTED STREAMS.
963 *Water Resources Research*, *52*(5), 3910–3929. https://doi.org/10.1002/2015WR018306
964 Livers, B., Wohl, E., Jackson, K. J., & Sutfin, N. A. (2018). Historical land use as a driver of alternative
965 states for stream form and function in forested mountain watersheds of the Southern Rocky
966 Mountains. *Earth Surface Processes and Landforms*, *43*(3), 669–684.
967 https://doi.org/10.1002/esp.4275
968 Lynch, L. M., Machmuller, M. B., Boot, C. M., Covino, T. P., Rithner, C. D., Cotrufo, M. F., et al. (2019).
969 Dissolved organic matter chemistry and transport along an Arctic tundra hillslope. *Global*
970 *Biogeochemical Cycles*.
971 Lynch, L. M., Sutfin, N. A., Fegel, T. S., Boot, C. M., Covino, T. P., & Wallenstein, M. D. (2019). River
972 channel connectivity shifts metabolite composition and dissolved organic matter chemistry.
973 *Nature Communications*, *10*(1), 459. https://doi.org/10.1038/s41467-019-08406-8
974 Manga, M., & Kirchner, J. W. (2000). Stress partitioning in streams by large woody debris. *Water*
975 *Resources Research*, *36*(8), 2373–2379. https://doi.org/10.1029/2000WR900153
976 McCain, J. F., & Shroba, R. R. (1979). *Storm and flood of July 31-August 1, 1976, in the Big Thompson*
977 *River and Cache la Poudre River basins, Larimer and Weld Counties, Colorado* (USGS Numbered
978 Series No. 1115- A,B). U.S. Govt. Print. Off.,. Retrieved from
979 http://pubs.er.usgs.gov/publication/pp1115AB
980 Montgomery, D. R., & Buffington, J. M. (1997). Channel-reach morphology in mountain drainage basins.
981 *GSA Bulletin*, *109*(5), 596–611. https://doi.org/10.1130/0016-
982 7606(1997)109<0596:CRMIMD>2.3.CO;2
983 Moody, J. A., & Ebel, B. A. (2012). Hyper-dry conditions provide new insights into the cause of extreme
984 floods after wildfire. *CATENA*, *93*, 58–63. https://doi.org/10.1016/j.catena.2012.01.006

985 Omengo, F. O., Geeraert, N., Bouillon, S., & Govers, G. (2018). Deposition and fate of organic carbon in
986 floodplains along a tropical semiarid lowland river (Tana River, Kenya). *Journal of Geophysical*
987 *Research: Biogeosciences*, 1131–1143.
988 https://doi.org/10.1002/2015JG003288@10.1002/(ISSN)2169-8961.CNFLOI1
989 Poff, N. L., Allan, J. D., Bain, M. B., Karr, J. R., Prestegaard, K. L., Richter, B. D., et al. (1997). The Natural
990 Flow Regime. *BioScience*, *47*(11), 769–784. https://doi.org/10.2307/1313099
991 Polvi, L. E., & Wohl, E. (2012). The beaver meadow complex revisited – the role of beavers in post-glacial
992 floodplain development. *Earth Surface Processes and Landforms*, *37*(3), 332–346.
993 https://doi.org/10.1002/esp.2261
994 Polvi, L. E., & Wohl, E. (2013). Biotic Drivers of Stream PlanformImplications for Understanding the Past
995 and Restoring the Future. *BioScience*, *63*(6), 439–452. https://doi.org/10.1525/bio.2013.63.6.6
996 Polvi, L. E., Wohl, E. E., & Merritt, D. M. (2011). Geomorphic and process domain controls on riparian
997 zones in the Colorado Front Range. *Geomorphology*, *125*(4), 504–516.
998 https://doi.org/10.1016/j.geomorph.2010.10.012
999 PRISM Climate Group. (2012). *Oregon State University*. Retrieved from http://prism.oregonstate.edu
1000 Quinn, J. M., Phillips, N. R., & Parkyn, S. M. (2007). Factors influencing retention of coarse particulate
1001 organic matter in streams. *Earth Surface Processes and Landforms*, *32*(8), 1186–1203.
1002 https://doi.org/10.1002/esp.1547
1003 R Core Team. (2017). *R: A language and environment for statistical computing*. Vienna, Austria: R
1004 Foundation for Statistical Computing. Retrieved from http://www.R-project.org/
1005 Rathburn, S. L., Bennett, G. L., Wohl, E. E., Briles, C., McElroy, B., & Sutfin, N. (2017). The fate of
1006 sediment, wood, and organic carbon eroded during an extreme flood, Colorado Front Range,
1007 USA. *Geology*, *45*(6), 499–502. https://doi.org/10.1130/G38935.1

1008 Raymond, P. A., Saiers, J. E., & Sobczak, W. V. (2016). Hydrological and biogeochemical controls on
1009 watershed dissolved organic matter transport: pulse-shunt concept. *Ecology*, *97*(1), 5–16.
1010 https://doi.org/10.1890/14-1684.1
1011 Richter, B. D., Baumgartner, J. V., Powell, J., & Braun, D. P. (1996). A Method for Assessing Hydrologic
1012 Alteration within Ecosystems. *Conservation Biology*, *10*(4), 1163–1174.
1013 https://doi.org/10.1046/j.1523-1739.1996.10041163.x
1014 Ricker, M. C., & Lockaby, B. G. (2015). Soil Organic Carbon Stocks in a Large Eutrophic Floodplain Forest
1015 of the Southeastern Atlantic Coastal Plain, USA. *Wetlands*, *35*(2), 291–301.
1016 https://doi.org/10.1007/s13157-014-0618-y
1017 Sear, D. A., Millington, C. E., Kitts, D. R., & Jeffries, R. (2010). Logjam controls on channel:floodplain
1018 interactions in wooded catchments and their role in the formation of multi-channel patterns.
1019 *Geomorphology*, *116*(3), 305–319. https://doi.org/10.1016/j.geomorph.2009.11.022
1020 Sharma, A., Wasko, C., & Lettenmaier, D. P. (2018). If Precipitation Extremes Are Increasing, Why Aren't
1021 Floods? *Water Resources Research*, *54*(11), 8545–8551.
1022 https://doi.org/10.1029/2018WR023749
1023 Sholtes, J. S., Yochum, S. E., Scott, J. A., & Bledsoe, B. P. (2018). Longitudinal variability of geomorphic
1024 response to floods. *Earth Surface Processes and Landforms*, *43*(15), 3099–3113.
1025 https://doi.org/10.1002/esp.4472
1026 Simon, A., & Collison, A. J. C. (2002). Quantifying the mechanical and hydrologic effects of riparian
1027 vegetation on streambank stability. *Earth Surface Processes and Landforms*, *27*(5), 527–546.
1028 https://doi.org/10.1002/esp.325
1029 Stegen, J. C., Fredrickson, J. K., Wilkins, M. J., Konopka, A. E., Nelson, W. C., Arntzen, E. V., et al. (2016).
1030 Groundwater–surface water mixing shifts ecological assembly processes and stimulates organic
1031 carbon turnover. *Nature Communications*, *7*(1), 11237. https://doi.org/10.1038/ncomms11237

1032 Stewart, I. T. (2009). Changes in snowpack and snowmelt runoff for key mountain regions. *Hydrological*
1033 *Processes*, *23*(1), 78–94. https://doi.org/10.1002/hyp.7128
1034 Sutfin, N. (2020, May 28). Floodplain organic carbon storage along streams in the Colorado Front Range,
1035 U.S.A. https://doi.org/10.6084/m9.figshare.12014586.v1
1036 Sutfin, N. A., & Wohl, E. (2017). Substantial soil organic carbon retention along floodplains of mountain
1037 streams. *Journal of Geophysical Research: Earth Surface*, *122*(7), 1325–1338.
1038 https://doi.org/10.1002/2016JF004004
1039 Sutfin, N. A., & Wohl, E. (2019). Elevational differences in hydrogeomorphic disturbance regime
1040 influence sediment residence times within mountain river corridors. *Nature Communications*,
1041 *10*(1), 2221. https://doi.org/10.1038/s41467-019-09864-w
1042 Sutfin, N. A., Wohl, E. E., & Dwire, K. A. (2016). Banking carbon: a review of organic carbon storage and
1043 physical factors influencing retention in floodplains and riparian ecosystems. *Earth Surface*
1044 *Processes and Landforms*, *41*(1), 38–60. https://doi.org/10.1002/esp.3857
1045 Tabari, H. (2020). Climate change impact on flood and extreme precipitation increases with water
1046 availability. *Scientific Reports*, *10*(1), 13768. https://doi.org/10.1038/s41598-020-70816-2
1047 Vannote, R. L., Minshall, G. W., Cummins, K. W., Sedell, J. R., & Cushing, C. E. (1980). The River
1048 Continuum Concept. *Canadian Journal of Fisheries and Aquatic Sciences*, *37*(1), 130–137.
1049 https://doi.org/10.1139/f80-017
1050 Veblen, T. T., & Donnegan, J. (2005). *Historical Range of Variability for Forest Vegetation of the National*
1051 *Forests of the Colorado Front Range* (p. 154). Golden, CO: USDA Forest Service, Rocky Mountain
1052 Region.
1053 Venarsky, M. P., Walters, D. M., Hall, R. O., Livers, B., & Wohl, E. (2018). Shifting stream planform state
1054 decreases stream productivity yet increases riparian animal production. *Oecologia*, *187*(1), 167–
1055 180. https://doi.org/10.1007/s00442-018-4106-6

1056 Weishaar, J. L., Aiken, G. R., Bergamaschi, B. A., Fram, M. S., Fujii, R., & Mopper, K. (2003). Evaluation of
1057 Specific Ultraviolet Absorbance as an Indicator of the Chemical Composition and Reactivity of
1058 Dissolved Organic Carbon. *Environmental Science & Technology*, *37*(20), 4702–4708.
1059 https://doi.org/10.1021/es030360x
1060 Wohl, E. (2008). The effect of bedrock jointing on the formation of straths in the Cache la Poudre River
1061 drainage, Colorado Front Range. *Journal of Geophysical Research: Earth Surface*, *113*(F1).
1062 https://doi.org/10.1029/2007JF000817
1063 Wohl, E. (2013). Landscape-scale carbon storage associated with beaver dams. *Geophysical Research*
1064 *Letters*, *40*(14), 3631–3636. https://doi.org/10.1002/grl.50710
1065 Wohl, E., Dwire, K., Sutfin, N., Polvi, L., & Bazan, R. (2012). Mechanisms of carbon storage in
1066 mountainous headwater rivers. *Nature Communications; London*, *3*, 1263.
1067 http://dx.doi.org/10.1038/ncomms2274
1068 Wohl, E., Bledsoe, B. P., Jacobson, R. B., Poff, N. L., Rathburn, S. L., Walters, D. M., & Wilcox, A. C. (2015).
1069 The Natural Sediment Regime in Rivers: Broadening the Foundation for Ecosystem
1070 Management. *BioScience*, *65*(4), 358–371. https://doi.org/10.1093/biosci/biv002
1071 Wohl, E., Lininger, K. B., & Scott, D. N. (2017). River beads as a conceptual framework for building carbon
1072 storage and resilience to extreme climate events into river management. *Biogeochemistry*, 1–
1073 19. https://doi.org/10.1007/s10533-017-0397-7
1074 Wollheim, W. M., Bernal, S., Burns, D. A., Czuba, J. A., Driscoll, C. T., Hansen, A. T., et al. (2018). River
1075 network saturation concept: factors influencing the balance of biogeochemical supply and
1076 demand of river networks. *Biogeochemistry*, *141*(3), 503–521. https://doi.org/10.1007/s10533-
1077 018-0488-0
1078 Yochum, S. E., & Collins, F. (2015). COLORADO FRONT RANGE FLOOD OF 2013: PEAK FLOWS AND FLOOD
1079 FREQUENCIES, 12.

Yochum, S. E., Sholtes, J. S., Scott, J. A., & Bledsoe, B. P. (2017). Stream power framework for predicting geomorphic change: The 2013 Colorado Front Range flood. *Geomorphology*, *292*, 178–192. https://doi.org/10.1016/j.geomorph.2017.03.004

Figure 1. Map of the study area along the Colorado Front Range of the Rocky Mountains, U.S. Twenty-four study reaches representing five different channel types (A) are indicated in the legend. Large rectangles with bold outlines identify intensive study sites that capture transitions in channel complexity (single-multiple-single thread reaches) on Glacier Creek (B) and Ouzel Creek (C). At these intensive study sites, organic matter composition was examined along transitions in valley confinement using fluorescence spectroscopy. Logjam surveys were conducted in the N. Saint Vrain Creek Basin upstream of the Rocky Mountain National Park boundary.

Figure 2. Bar plots of OC storage per area. 24 study reaches are represented by five valley types that vary by degree of confinement and channel complexity. (A) TOC (total OC) is the sum of combined OC stored in (i) litter, (ii) large wood, and (iii) floodplain fine sediment and soil. (B) The zoomed in area of OC storage as wood and litter using a different scale provides details of differences between channel type. Letters a and b indicate group assignments for channel types within each OC reservoir (based on statistical significance at the 95% confidence level using Tukey HSD pairwise comparisons). Channel types sharing any combination of a or b are not significantly different, whereas channel types that do not share a common letter are significantly different.

Figure 3. Boxplots of floodplain soil depth and mean soil organic carbon content (OC) by valley type. Letters *a* and *b* indicate group assignments for channel types within each OC reservoir (based on statistical significance at the 95% confidence level using Tukey HSD pairwise

comparisons). Channel types sharing any combination of a or b are not significantly different, whereas channel types that do not share a common letter are significantly different.

Figure 4. Principal components analysis (PCA) of FDOM composition (A, B) and a diagram illustrating results as a function of channel complexity (C). The contribution (in percent) of individual variables (vector shade) and samples (symbol size) to principal components 1 and 2 are shown for (A) surface waters and (B) soil leachates (data provided in Table S7). Shaded ellipses correspond to 95% confidence intervals for the upper confined (red), lower confined (blue), and middle multithread (yellow) reaches. The diagram (C) depicts two sampling transects within each reach (colors match PCA plots).

Table 1

Physical attributes of the 24 study reaches.

Table 2

Floodplain organic carbon storage in litter, large wood, and soil + fine sediment among all study reaches.

Table 3 Stepwise regression transformations and results